

Measurement of the Saturation Length of the Self-Modulation Instability

A. Clairembaud,¹ M. Turner,² M. Bergamaschi,² L. Ranc,¹ F. Pannell,³
 J. Mezger,¹ H. Jaworska,² N. van Gils,^{2,4} J. Farmer,¹ and P. Muggli^{1,2}
 (AWAKE Collaboration)

C.C. Ahdida,² Y. Alekajbaf,⁵ C. Amoedo,² O. Apsimon,^{6,7} R. Apsimon,^{7,8} T. Bachmann,² C. Badiali,⁹
 M. Baquero,¹⁰ E. Belli,^{2,11} A. Boccardi,² T. Bogey,² S. Burger,² P.N. Burrows,¹¹ B. Buttenschön,¹² A. Caldwell,¹
 M. Chung,¹³ C.C. Cobo,¹⁴ D.A. Cooke,³ D. Dancila,⁵ C. Davut,^{6,7} G. Demeter,¹⁵ A.C. Dexter,^{7,8}
 S. Doeberl,² A. Eager,² D. Easton,¹⁶ B. Elward,¹⁷ R. Fonseca,^{18,9} I. Furno,¹⁰ K. Gajewski,⁵ D. Ghosal,^{7,19}
 E. Granados,² J. Gregory,^{7,8} O. Grulke,^{12,20} E. Gschwendtner,² E. Guran,² D. Harryman,² M. Hibberd,^{6,7}
 P. Karataev,^{11,21} R. Karimov,¹⁰ M.A. Kedves,¹⁵ F. Kraus,²² M. Krupa,² T. Lefevre,² T. Lofnes,⁵ N. Lopes,⁹
 K. Lotov, J. Mcgunigal,^{6,7} S.A. Mohadeskasaei,⁵ M. Moreira,² B. Moser,² Z. Najmudin,¹⁴ S. Norman,^{6,7}
 N. Okhotnikov, A. Omoumi,² C. Pakuza,² A. Pardons,² K. Pelckmans,⁵ J. Pisani,¹⁶ A. Pukhov,²³ R. Rossel,²
 H. Saberi,^{6,7} M.V. dos Santos,² O. Schmitz,¹⁷ F. Sharmin,¹⁷ F. Silva,²⁴ L. Silva,⁹ B. Spear,¹¹ L. Stant,²
 C. Stollberg,¹⁰ A. Sublet,² C. Swain,^{7,19} G. Tenasini,² A. Topaloudis,² P. Tuev, J. Uncles,¹⁶ F. Velotti,² J. Vieira,⁹
 C. Welsch,^{7,19} T. Wilson,²³ M. Wing,³ J. Wolfenden,^{7,19} B. Woolley,² G. Xia,^{7,6} V. Yarygova, and W. Zhang¹¹

¹Max Planck Institute for Physics, 85748 Garching bei München, Germany

²CERN, 1211 Geneva 23, Switzerland

³UCL, London WC1E 6BT, United Kingdom

⁴PARTREC, UMCG, University of Groningen, Groningen, NL

⁵Uppsala University, Uppsala, Sweden

⁶University of Manchester, Manchester M13 9PL, United Kingdom

⁷Cockcroft Institute, Warrington WA4 4AD, United Kingdom

⁸Lancaster University, Lancaster LA1 4YB, United Kingdom

⁹GoLP/Instituto de Plasmas e Fusão Nuclear, Instituto Superior Técnico,

Universidade de Lisboa, 1049-001 Lisbon, Portugal

¹⁰Ecole Polytechnique Federale de Lausanne (EPFL),

Swiss Plasma Center (SPC), 1015 Lausanne, Switzerland

¹¹John Adams Institute, Oxford University, Oxford OX1 3RH, United Kingdom

¹²Max Planck Institute for Plasma Physics, 17491 Greifswald, Germany

¹³POSTECH, Pohang 37673, Republic of Korea

¹⁴Imperial College London, London SW7 2AZ, United Kingdom

¹⁵HUN-REN Wigner Research Centre for Physics, Budapest, Hungary

¹⁶GWA, Cambridge, CB4 0WS UK

¹⁷University of Wisconsin, Madison, WI 53706, USA

¹⁸DCTI/ISCTE, Instituto Universitário de Lisboa, 1649-026, Lisboa, Portugal

¹⁹University of Liverpool, Liverpool L69 7ZE, United Kingdom

²⁰Technical University of Denmark, 2800 Kgs. Lyngby, Denmark

²¹Royal Holloway University of London, Egham, Surrey, TW20 0EX, United Kingdom

²²Universität Bonn, 53121 Bonn, Germany

²³Heinrich-Heine-Universität Düsseldorf, 40225 Düsseldorf, Germany

²⁴INESC-ID, Instituto Superior Técnico, Universidade de Lisboa, 1049-001 Lisbon, Portugal

(Dated: February 19, 2026)

The self-modulation (SM) instability transforms a long charged particle bunch traveling in plasma into a train of microbunches that resonantly drives large-amplitude wakefields. We present the first determination of the saturation length of SM using experimental and numerical results. The saturation length is the distance over which wakefields reach their maximum amplitude along the plasma. By varying the plasma length and measuring the radius of the transverse distribution of the bunch, we find that the saturation length of SM decreases with plasma density and initial field amplitude, e.g., when seeding. The saturation length is a fundamental parameter of the instability, and these results are key for understanding SM and designing plasma wakefield accelerators driven by long bunches, such as AWAKE, or by long laser pulses for radiation production.

Introduction – Instabilities play a central role in plasma physics (see, e.g., Ref. [1]). In particular, understanding their development and saturation is essential. A fundamental parameter characterizing many instabilities is the

saturation length. An instability can grow in space from an initially small (linear) amplitude. Growth leads to nonlinear effects, and at the saturation length the amplitude reaches a large and essentially constant value, lim-

ited by these effects. In general, the effect sought after is maximum at saturation, and its event-to-event variations are also smaller than during growth.

For example, in free electron lasers (FELs), a particle bunch modulates to emit light with exponentially growing intensity. The saturation length, L_{sat} , can be determined by measuring the radiation power as a function of undulator length (see e.g., Ref. [2]). Determining L_{sat} is crucial, as it sets the minimum undulator length required for the FEL to reach maximum output power.

In plasma, an analogous microbunching process occurs in the self-modulation (SM) instability of a relativistic charged particle bunch. SM develops when the duration of the bunch σ_t is much longer than the plasma electron period τ_{pe} [3]. It has been observed with electron [4–6] and proton [7] bunches. SM also occurs with long laser pulses propagating in plasmas [8–10] and has been observed in experiments [11]. Despite these observations, the saturation length of SM has not yet been measured experimentally.

The initial transverse wakefields driven by the long bunch have small amplitude and periodically modulate the bunch density with period τ_{pe} . Since the modulated bunch drives higher-amplitude wakefields, a feedback loop between density modulation and wakefields is set up. This leads to growth of SM along the plasma and along the bunch. The growth saturates when the bunch is fully modulated, i.e., when the resulting train of microbunches resonantly excites wakefields to the highest amplitudes.

Unlike in FELs, where radiation power can be measured directly, wakefield amplitudes are difficult to measure [12]. It is therefore necessary to rely on indirect effects of the wakefields to determine the saturation length of SM.

Because SM is a transverse process, the formation of the microbunch train leads to that of a halo of defocused particles surrounding the train. This halo formation is both the cause (modulation of the bunch density) and a consequence (effect of transverse wakefields) of the growth of the wakefields along the plasma [13]. One can expect the formation process to slow significantly once the microbunch train is fully formed, and when saturation of SM is reached, at L_{sat} . This key parameter can therefore be experimentally determined by characterizing the evolution of the halo of defocused particles along the plasma [14].

In this *Letter*, we determine for the first time, with experimental and numerical simulation results, the saturation length of the SM process. By varying the plasma length and measuring the radius of the halo at a screen downstream of the plasma, we identify the distance over which this radius increases and saturates as a function of experimental parameters. We find that the saturation length of the radius decreases with increasing plasma electron density, and that seeding the SM process makes this length shorter than in the non-seeded case. Numerical simulation results indicate that the saturation length

of the halo radius provides a good estimate for that of SM. There is excellent agreement between numerical simulation and experimental results for the saturation length of the halo radius.

Experimental Setup — Measurements were performed in the context of AWAKE (Advanced WAKEfield Experiment) at CERN [15]. A schematic layout of the experiment is shown on Fig. 1.

A 400 GeV proton bunch from the Super Proton Synchrotron, with a population $N_b \cong 3 \times 10^{11}$ particles, is focused to an rms transverse size $\sigma_r \cong 200 \mu\text{m}$ at the entrance of the plasma. The bunch has a normalized emittance $\epsilon_N \cong 2.2 \text{ mm-mrad}$, and an rms duration $\sigma_t \cong 170 \text{ ps}$.

A short laser pulse with FWHM duration 120 fs and energy $\sim 100 \text{ mJ}$ co-propagates with the proton bunch. It forms a relativistic ionization front (RIF), and ionizes a rubidium vapor ($\text{RbI} \rightarrow \text{RbII}$), resulting in a plasma electron density n_{pe} that can be varied in the range $\cong (1 - 10) \times 10^{14} \text{ cm}^{-3}$ [16]. This range of densities corresponds to plasma periods much shorter than the bunch duration ($\tau_{pe} = 2\pi\sqrt{\frac{m_e\epsilon_0}{n_{pe}e^2}} \cong (11 - 3) \text{ ps} \ll \sigma_t \cong 170 \text{ ps}$), enabling the development of SM. When placed within the bunch, the RIF defines the onset of the beam-plasma interaction, and thus the timing and amplitude of the initial wakefields that can seed SM [17].

The laser pulse propagation can be stopped at different locations along the 10.3 m-long vapor column by inserting a thin (200 μm) aluminum foil (laser blocks on Fig. 1). The plasma length (L_p) over which the proton bunch propagates can therefore be varied ($L_p = 0.5, 1.5, \dots, 9.5 \text{ m}$), and thus also the distance over which SM develops.

To observe the development of SM along the plasma, we record the transverse profile of the bunch on a scintillating screen as a function of L_p . The screen is placed 20.3 m downstream from the plasma entrance, and a camera images the light emitted by the screen after the passage of the bunch. Since the energy spread of the proton bunch caused by interaction with the wakefields is

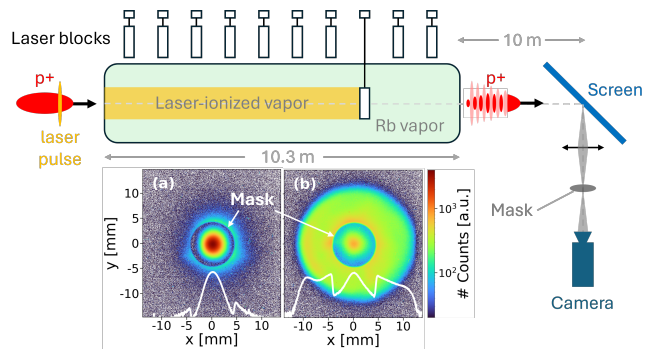


FIG. 1. Schematic of the experimental setup (not to scale). Inset: Transverse distribution of the bunch at the screen for single events after propagating through (a) Rubidium vapor, (b) 9.5 m of plasma. Colormap: logarithmic scale.

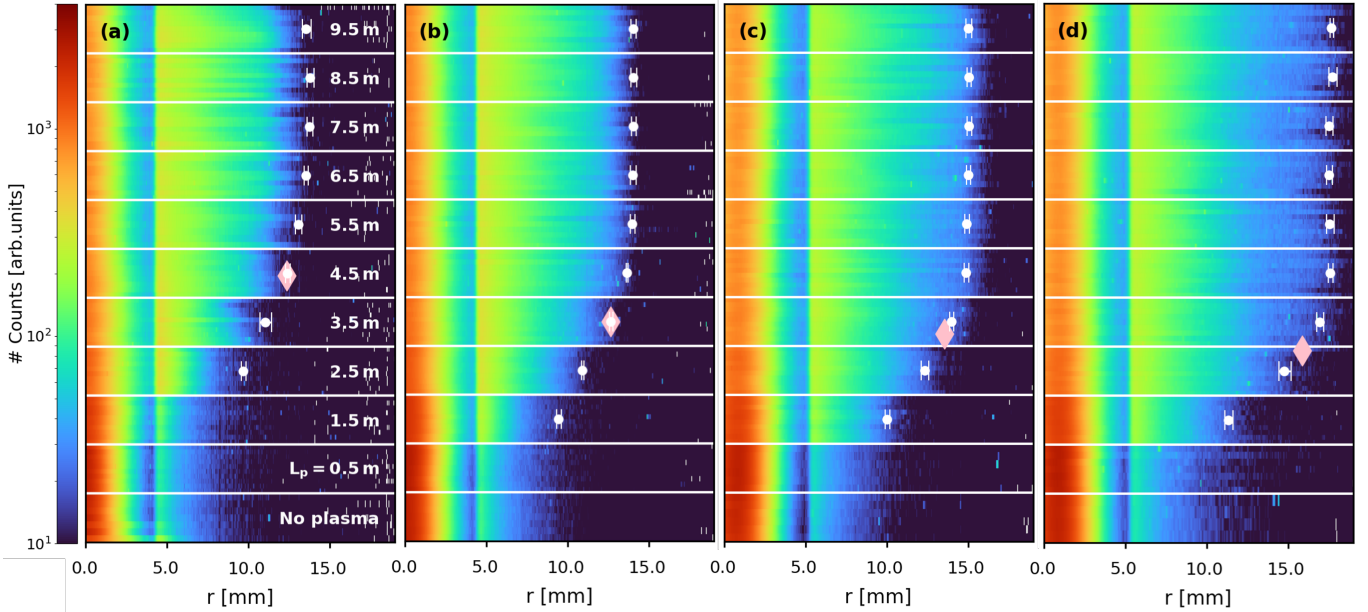


FIG. 2. Radial slices of the transverse distribution of the bunch at the screen for different propagation distances in plasma (L_p). (a) $n_{pe} = (1.06 \pm 0.01) \times 10^{14} \text{ cm}^{-3}$, (b) $(1.98 \pm 0.01) \times 10^{14} \text{ cm}^{-3}$, (c) $(3.90 \pm 0.02) \times 10^{14} \text{ cm}^{-3}$, (d) $(7.42 \pm 0.03) \times 10^{14} \text{ cm}^{-3}$. Colormap: logarithmic scale. White symbols: average radius of the halo r_h for the corresponding L_p , error bars: standard deviation of ~ 10 events. Pink diamonds: saturation point of the radius ($r_h = 0.9 r_{h,\text{max}}$). $t_{\text{RIF}} = 100 \text{ ps}$ ($\sim 0.6\sigma_t$). (a) $N_b = (2.98 \pm 0.08) \times 10^{11}$, (b) $(2.98 \pm 0.03) \times 10^{11}$, (c) $(2.86 \pm 0.05) \times 10^{11}$, (d) $(2.87 \pm 0.05) \times 10^{11}$.

small ($\Delta E/E < 2.5\%$), the number of counts per pixel recorded by the camera is proportional to the local, time-integrated proton bunch density. A circular attenuating mask with transmission 17% and radius 4 mm is placed in an image plane of the optical line of the camera, and approximately aligned with the center of the bunch (Inset (a), Fig. 1). This enables simultaneous observation of the faint halo of defocused particles and of the intense bunch core formed by the train, without saturating the 12-bit camera.

Results – The inset of Fig. 1 shows time-integrated transverse profiles of the bunch at the screen after propagation (a) in vapor (no laser pulse), and (b) in a plasma with $L_p = 9.5 \text{ m}$. When propagating in vapor, the unmodulated bunch fits entirely under the mask and has a Gaussian-like distribution (Inset (a)). After propagating in plasma, the bunch exhibits a halo, indicating that SM has developed [13] (Inset (b)). The halo distribution has a sharp outer edge, the radius of which, r_h , can be accurately determined following the procedure described in Ref. [18].

We extract a horizontal slice of the distribution of ~ 10 successive events for each value of L_p , and plot them consecutively on Fig. 2 for four values of n_{pe} . The instability is seeded, thus ensuring that the process is reproducible from event to event, as shown by the small variations of r_h . Under these conditions, varying L_p is equivalent to observing the state of the bunch (and related wakefields) at different locations along the plasma for a single SM event.

The evolution of the bunch distribution (discussed below for Fig. 2(d)) can be divided into three distinct phases.

During the first phase, from $L_p = 0$ to 0.5 m , the seed fields driven by the unmodulated bunch have small amplitude (few MV/m) [13, 17], and are predominantly focusing [19, 20]. Since the relativistic protons ($\gamma_0 = 427$) have a large inertia, very little transverse evolution occurs over this short distance in plasma (compare with “No plasma”).

During the second phase, occurring from $L_p = 0.5$ to 3.5 m , the periodic, transverse wakefields develop alternating focusing and defocusing regions. As a result, a fraction of the protons are defocused and leave the wakefields transversely, thus forming the halo surrounding the bunch core. This is seen on the image as an increase in charge density at large radii ($r > 4 \text{ mm}$, i.e., beyond the mask) and as a simultaneous decrease under the mask, and thus to an increase in r_h , as expected. The observation of the formation of the halo with L_p clearly indicates that SM is growing within this section of plasma. We quantify the evolution by measuring the average radius $r_{h,\text{avg}}$ (white symbols), e.g., with an increase from $r_{h,\text{avg}} = 11.3$ to 16.9 mm for $L_p = 1.5$ to 3.5 m .

During the third phase, occurring from $L_p = 3.5$ to 9.5 m , the transverse distribution of the bunch remains essentially unchanged, and r_h has saturated at its maximum value $r_{h,\text{max}}$. This is the signature expected from saturation of the SM process. We note that for these L_p , time-resolved images of the bunch (not shown) ex-

hibit deep modulation of the longitudinal bunch density, another signature of the saturation of SM [3, 21].

We define the saturation length of the halo radius L_{sat} as the interpolated L_p at which r_h reaches $0.9 r_{h,\text{max}}$: a threshold chosen to enable reliable determination of L_{sat} , i.e., before the growth curve flattens and r_h becomes weakly dependent on L_p . It is indicated by the pink diamonds on Fig. 2. These clearly indicate the decrease of L_{sat} with increasing n_{pe} ((4.5 ± 0.2) m, to (2.9 ± 0.1) m from Figs. 2(a) to (d)).

To determine whether the saturation length of the halo radius provides an estimate for that of SM, we perform 2D axisymmetric particle-in-cell simulations using LCODE [22] with parameters similar to those of the experiments. We propagate ballistically the bunch phase space distribution at the end of the plasma L_p to a location equivalent to that of the screen in the experiment. This produces transverse proton distributions that can be compared to those obtained in the experiment, e.g., Figs. 1(a) and (b). We determine the halo radius and the saturation length from these propagated distributions,

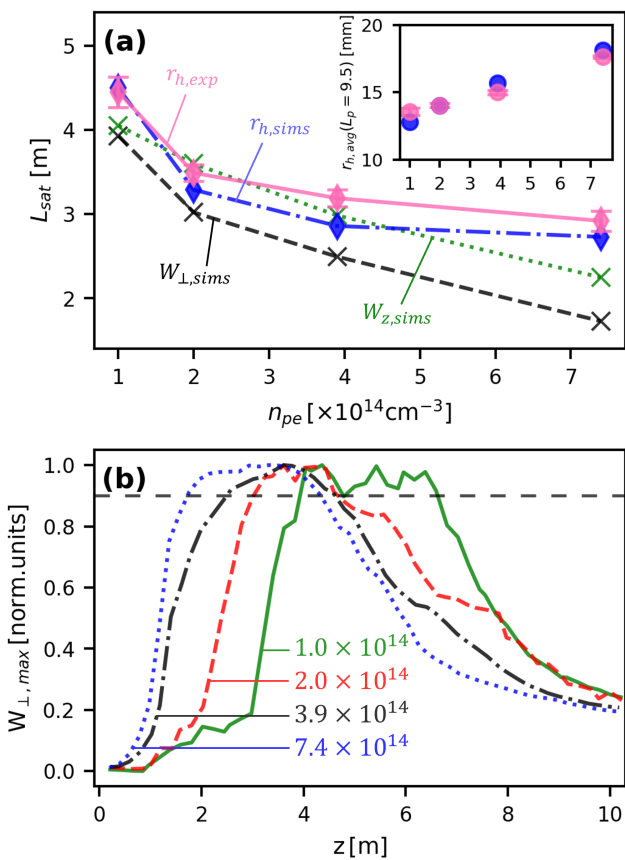


FIG. 3. (a) Saturation length L_{sat} as a function of n_{pe} (same values as on Fig. 2) labeled with the quantity it is determined from. Inset: $r_{h,\text{avg}}(L_p = 9.5 \text{ m})$ as a function of $n_{pe} [\times 10^{14} \text{ cm}^{-3}]$. (b) Normalized transverse wakefield amplitude $W_{\perp,\text{max}}$ along the plasma for the four n_{pe} values of Fig. 2. Black dashed line: 90% of peak value.

using the same procedure as for the experimental images.

The inset of Fig. 3(a) shows close agreement between experimental (pink symbols) and numerical simulation (blue symbols) results for $r_{h,\text{avg}}(L_p = 9.5 \text{ m})$, with differences below 1 mm for radii of more than 12 mm. The figure shows that the corresponding experimental and simulation saturation lengths of r_h are also in very good agreement, with differences of less than 0.5 m. These small differences may be due to differences in the exact input parameters between numerical simulations and experiments [23], namely bunch transverse size and emittance [24].

Numerical simulation results also provide the amplitude of the transverse wakefields W_{\perp} that lead to the formation of the halo. Their amplitude varies along the bunch, and we plot on Fig. 3(b) their maximum amplitude as a function of position along the plasma, evaluated at $r = c/\omega_{pe}$ (the plasma electron collisionless skin depth with $\omega_{pe} = 2\pi/\tau_{pe}$), and in the front of the bunch ($-\sigma_t < t < t_{\text{RIF}}$, where $t = 0$ is the bunch center). Simulation results show that this temporal extent of the bunch corresponds to the origin of the most defocused protons, i.e., those that define the halo radius. In the context of a plasma wakefield accelerator, this extent also corresponds to the location in the wakefields along the bunch where a witness bunch would be injected for acceleration [25]. The field amplitudes are normalized to their maximum value to facilitate comparison of their development for different values of n_{pe} . In all cases, the wakefields grow, saturate, and then decay, which is typical of the development of SM along a plasma with constant density [3, 26]. It is clear from Fig. 3(b) that the development of SM occurs earlier with larger n_{pe} , as expected [21]. For consistency, we define the saturation length of the wakefields (and thus of SM) as the location where their amplitude reaches 90% of their maximum value. We plot the saturation length of the wakefields on the same plot as that of the halo radius (black symbols on Fig. 3(a)). Although not the cause of the bunch halo, we apply the same analysis procedure to the longitudinal wakefields $W_z = E_z$ ($r = 0$, and accelerating for electrons), and also plot their saturation length on Fig. 3(a) (green symbols).

Figure 3(a) shows that the three saturation lengths follow the same trend versus n_{pe} and remain close in value, although W_{\perp} saturate earlier. The difference between L_{sat} inferred from r_h and from W_{\perp} may be due to the fact that, after saturation, the continuous backward shift of the wakefields, with phase velocity slower than that of the protons [21, 27], leads to further evolution of the SM process (see Fig. 3(b)). As a result, protons from the microbunch train may enter the defocusing regions of the wakefields, gain additional transverse momentum, and exit the wakefields transversely. Because these defocused protons experience the largest field amplitudes, i.e., those near saturation, they reach the largest radii at the screen. This causes the halo radius to saturate slightly later than W_{\perp} , while still tracking its saturation length. Further along the plasma, the wakefield amplitude drops

significantly, and protons shed by the backward shift of the wakefields do not acquire enough momentum to reach larger radii [14].

Overall, the results of Fig. 3(a) show that measuring the saturation length of the halo radius gives a good estimate of the saturation length of SM. This method can therefore be used to determine L_{sat} , a fundamental parameter of SM.

We next investigate the effect of the initial wakefield amplitude on the saturation length of SM. Since the initial wakefield amplitude scales with the local bunch density n_b at the RIF [17, 19], it can be varied by changing the timing of the RIF along the bunch.

Here, we compare the evolution of SM for $t_{\text{RIF}} = 350$ ps (Fig. 4(a)) and $t_{\text{RIF}} = 550$ ps (Fig. 4(b)). These t_{RIF} values are chosen such that the bunch charge in plasma (i.e., after the RIF) remains similar in the two cases (difference $< 2.5\%$), ensuring that the dominant varying parameter is the initial field amplitude, and not the growth rate [3, 21, 27]. For $t_{\text{RIF}} = 550$ ps, the initial field amplitude induced by the RIF is lower than for $t_{\text{RIF}} = 350$ ps ($W_{\perp,0}(t_{\text{RIF}}) \propto n_b(t_{\text{RIF}})$), and not sufficient to overcome the wakefields driven by noise or features in the bunch distribution. In this case, the SM process is no longer seeded and develops as an instability (SMI) [17, 28].

In the seeded self-modulation (SSM) case, the wakefields acquire defocusing regions and reach a high amplitude earlier along L_p , as shown on Fig. 4 by the halo of defocused protons appearing earlier along the plasma ($L_p \approx 3.5$ m, Fig. 4(a)) than in the SMI case ($L_p \approx 5.5$ m, Fig. 4(b)). Although the variations in initial field amplitude and asymmetries in the modulated bunch structure are larger in the case of SMI (visible on the images, not

shown here), the radius of the halo also grows and saturates, as shown by the average radius values (white symbols in Fig. 4(b)). Following the same procedure as the one used on Fig. 3(a), we determine that the halo radius saturates at $L_{\text{sat}} = (4.9 \pm 0.2)$ m in the SSM case and $L_{\text{sat}} = (6.6 \pm 0.4)$ m in the SMI case, as indicated on Fig. 4 with pink diamonds. This result shows that seeding, i.e., providing higher initial field amplitude, reduces the saturation length of SM. This dependency is further supported by comparing $t_{\text{RIF}} = 100$ ps (Fig. 2(a)) and $t_{\text{RIF}} = 350$ ps (Fig. 4(a)), where saturation occurs earlier at $t_{\text{RIF}} = 100$ ps ($L_{\text{sat}} = (4.5 \pm 0.2)$ m vs (4.9 ± 0.2) m), i.e., when initial wakefields are larger, despite the lower bunch charge in plasma.

Figure 4 further shows that r_h is more reproducible from event to event in the SSM case than in the SMI case, e.g., with variations of 2.0% versus 4.6% (one standard deviation, shown with the error bars) for $L_p = 9.5$ m. This is consistent with timing reproducibility measurements of the microbunch train shown in the seeding demonstration experiments [17, 29], and will be the subject of another publication.

Summary & Conclusions – We have experimentally determined the saturation length of the self-modulation instability by measuring the evolution of the radius of the halo of defocused protons versus plasma length. We used numerical simulation results to show that saturation of the halo radius also corresponds to saturation of longitudinal and transverse wakefields, all three with similar saturation lengths. The saturation length decreases with increasing plasma electron density and initial field amplitude, e.g., when seeding. Understanding and measuring the characteristics of instabilities is key for validating theoretical models and numerical simulation results. For plasma-based accelerators driven by a long particle bunch using SM, measuring this length is crucial, as external injection must occur after saturation to maximize witness bunch energy and quality [27]. In particular, we have shown that SM saturates well within the 10 m of plasma foreseen for the length of the self-modulator in future acceleration experiments in AWAKE, which aims to produce high-energy electrons for particle physics applications [30–32]. Measuring the saturation length is also very important for plasma-based accelerators driven by long laser pulses developed as X-ray and γ -ray radiation sources [33, 34].

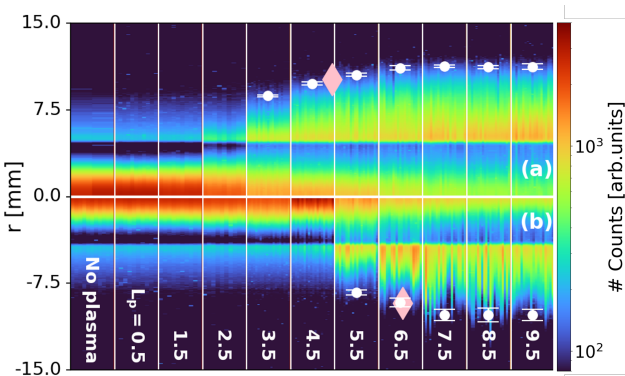


FIG. 4. Radial slices of the transverse distribution of the bunch at the screen for different propagation distance in plasma (L_p). (a) SSM ($t_{\text{RIF}} = 350$ ps ($\sim 2.1\sigma_t$)), (b) SMI ($t_{\text{RIF}} = 550$ ps ($\sim 3.2\sigma_t$)). Colormap: logarithmic scale. White symbols: average radius of the halo r_h for the corresponding L_p , error bars: standard deviation of ~ 20 events. Pink diamonds: saturation point of the radius ($r_h = 0.9 r_{h,\text{max}}$). (a) $n_{pe} = (1.02 \pm 0.01) \times 10^{14} \text{ cm}^{-3}$, $N_b = (2.92 \pm 0.02) \times 10^{11}$, (b) $n_{pe} = (1.08 \pm 0.01) \times 10^{14} \text{ cm}^{-3}$, $N_b = (2.87 \pm 0.02) \times 10^{11}$.

ACKNOWLEDGMENTS

This work was supported in parts by Fundação para a Ciência e Tecnologia–Portugal (Grant No. CERN/FIS TEC/0017/2019, No. CERN/FIS-TEC/0034/2021, No. UIDB/50021/2020); STFC (AWAKE-UK, Cockcroft Institute core, John Adams Institute core, and UCL consolidated grants), United Kingdom; the National Research Foundation of Korea (Grant No. NRF-2016R1A5A1013277 and No. NRF-2020R1A2C1010835).

M. W. acknowledges the support of DESY, Hamburg. Support of the Wigner Datacenter Cloud facility through the Awakelaser project is acknowledged. UW Madison

acknowledges support by NSF Award No. PHY-1903316. The AWAKE collaboration acknowledges the SPS team for their excellent proton delivery.

[1] Akira Hasegawa. *Plasma Instabilities and Nonlinear Effects*. Springer Berlin Heidelberg, 1975.

[2] Christoph Bostedt, Sébastien Boutet, David M. Fritz, Zhirong Huang, Hae Ja Lee, Henrik T. Lemke, Aymeric Robert, William F. Schlotter, Joshua J. Turner, and Garth J. Williams. Linac coherent light source: The first five years. *Rev. Mod. Phys.*, 88:015007, Mar 2016.

[3] Naveen Kumar, Alexander Pukhov, and Konstantin Lotov. Self-modulation instability of a long proton bunch in plasmas. *Phys. Rev. Lett.*, 104:255003, Jun 2010.

[4] Y. Fang, V. E. Yakimenko, M. Babzien, M. Fedurin, K. P. Kusche, R. Malone, J. Vieira, W. B. Mori, and P. Muggli. Seeding of self-modulation instability of a long electron bunch in a plasma. *Phys. Rev. Lett.*, 112:045001, Jan 2014.

[5] M. Gross, J. Engel, J. Good, H. Huck, I. Isaev, G. Koss, M. Krasilnikov, O. Lishilin, G. Loisch, Y. Renier, T. Rublack, F. Stephan, R. Brinkmann, A. Martinez de la Ossa, J. Osterhoff, D. Malyutin, D. Richter, T. Mehrling, M. Khojoyan, C. B. Schroeder, and F. Grüner. Observation of the self-modulation instability via time-resolved measurements. *Phys. Rev. Lett.*, 120:144802, Apr 2018.

[6] A. Del Dotto, A. C. Berceanu, A. Biagioni, M. Ferrario, G. Fortugno, R. Pompili, S. Romeo, A. R. Rossi, P. Santangelo, V. Shpakov, and A. Zigler. Experimental observation of the transition between hose and self-modulation instability regimes. *Physics of Plasmas*, 29(10):100701, 10 2022.

[7] E. Adli, A. Ahuja, O. Apsimon, R. Apsimon, A.-M. Bachmann, D. Barrientos, M. M. Barros, J. Batkiewicz, F. Batsch, J. Bauche, V. K. Berglyd Olsen, M. Bernardini, B. Biskup, A. Boccardi, T. Bogey, T. Bohl, C. Bracco, F. Braunmüller, S. Burger, G. Burt, S. Bustamante, B. Buttenschön, A. Caldwell, M. Cascella, J. Chappell, E. Chevallay, M. Chung, D. Cooke, H. Damerau, L. Deacon, L. H. Deubner, A. Dexter, S. Doeberl, J. Farmer, V. N. Fedosseev, G. Fior, R. Fiorito, R. A. Fonseca, F. Friebel, L. Garolfi, S. Gessner, I. Gorgisyan, A. A. Gorn, E. Granados, O. Grulke, E. Gschwendtner, A. Guerrero, J. Hansen, A. Helm, J. R. Henderson, C. Hessler, W. Hofle, M. Hüther, M. Ibisson, L. Jensen, S. Jolly, F. Keeble, S.-Y. Kim, F. Kraus, T. Lefevre, G. LeGodec, Y. Li, S. Liu, N. Lopes, K. V. Lotov, L. Maricalva Brun, M. Martyanov, S. Mazzoni, D. Medina Godoy, V. A. Minakov, J. Mitchell, J. C. Molendijk, R. Mompo, J. T. Moody, M. Moreira, P. Muggli, C. Mutin, E. Öz, E. Ozturk, C. Pasquino, A. Pardons, F. Peña Asmus, K. Pepitone, A. Perera, A. Petrenko, S. Pitman, G. Plyushchev, A. Pukhov, S. Rey, K. Rieger, H. Ruhl, J. S. Schmidt, I. A. Shalimova, E. Shaposhnikova, P. Sherwood, L. O. Silva, L. Soby, A. P. Sosedkin, R. Speroni, R. I. Spitsyn, P. V. Tuev, F. Velotti, L. Verra, V. A. Verzilov, J. Vieira, H. Vincke, C. P. Welsch, B. Williamson, M. Wing, B. Woolley, and G. Xia. Experimental observation of plasma wakefield growth driven by the seeded self-modulation of a proton bunch. *Phys. Rev. Lett.*, 122:054801, Feb 2019.

[8] Eric Esarey, Jonathan Krall, and Phillip Sprangle. Envelope analysis of intense laser pulse self-modulation in plasmas. *Phys. Rev. Lett.*, 72:2887–2890, May 1994.

[9] T. M. Antonsen and P. Mora. Self-focusing and raman scattering of laser pulses in tenuous plasmas. *Phys. Rev. Lett.*, 69:2204–2207, Oct 1992.

[10] P. Sprangle, E. Esarey, J. Krall, and G. Joyce. Propagation and guiding of intense laser pulses in plasmas. *Phys. Rev. Lett.*, 69:2200–2203, Oct 1992.

[11] A. Modena, Z. Najmudin, A. E. Dangor, C. E. Clayton, K. A. Marsh, C. Joshi, V. Malka, C. B. Darrow, C. Danson, D. Neely, and F. N. Walsh. Electron acceleration from the breaking of relativistic plasma waves. *Nature*, 377(6550):606–608, October 1995.

[12] Yang Wan, Sheroy Tata, Omri Seemann, Eitan Y Levine, Eyal Kroupp, and Victor Malka. Real-time visualization of the laser-plasma wakefield dynamics. *Science advances*, 10(5):eadj3595, 2024.

[13] M. Turner, E. Adli, A. Ahuja, O. Apsimon, R. Apsimon, A.-M. Bachmann, M. Barros Marin, D. Barrientos, F. Batsch, J. Batkiewicz, J. Bauche, V. K. Berglyd Olsen, M. Bernardini, B. Biskup, A. Boccardi, T. Bogey, T. Bohl, C. Bracco, F. Braunmüller, S. Burger, G. Burt, S. Bustamante, B. Buttenschön, A. Caldwell, M. Cascella, J. Chappell, E. Chevallay, M. Chung, D. Cooke, H. Damerau, L. Deacon, L. H. Deubner, A. Dexter, S. Doeberl, J. Farmer, V. N. Fedosseev, G. Fior, R. Fiorito, R. A. Fonseca, F. Friebel, L. Garolfi, S. Gessner, I. Gorgisyan, A. A. Gorn, E. Granados, O. Grulke, E. Gschwendtner, A. Guerrero, J. Hansen, A. Helm, J. R. Henderson, C. Hessler, W. Hofle, M. Hüther, M. Ibisson, L. Jensen, S. Jolly, F. Keeble, S.-Y. Kim, F. Kraus, T. Lefevre, G. LeGodec, Y. Li, S. Liu, N. Lopes, K. V. Lotov, L. Maricalva Brun, M. Martyanov, S. Mazzoni, D. Medina Godoy, V. A. Minakov, J. Mitchell, J. C. Molendijk, R. Mompo, J. T. Moody, M. Moreira, P. Muggli, E. Öz, E. Ozturk, C. Mutin, C. Pasquino, A. Pardons, F. Peña Asmus, K. Pepitone, A. Perera, A. Petrenko, S. Pitman, G. Plyushchev, A. Pukhov, S. Rey, K. Rieger, H. Ruhl, J. S. Schmidt, I. A. Shalimova, E. Shaposhnikova, P. Sherwood, L. O. Silva, L. Soby, A. P. Sosedkin, R. Speroni, R. I. Spitsyn, P. V. Tuev, F. Velotti, L. Verra, V. A. Verzilov, J. Vieira, H. Vincke, C. P. Welsch, B. Williamson, M. Wing, B. Woolley, and G. Xia. Experimental observation of plasma wakefield growth driven by the seeded self-modulation of a proton bunch. *Phys. Rev. Lett.*, 122:054801, Feb 2019.

[14] Arthur Clairembaud, Marlene Turner, and Patric Muggli. Development of self-modulation as a function of plasma length. *Nuclear Instruments and Methods in Physics Research Section A: Accelerators, Spectrometers, Detectors and Associated Equipment*, 1073:170265, 2025.

[15] Edda Gschwendtner, Konstantin Lotov, Patric Muggli, Matthew Wing, Riccardo Agnello, Claudia Christina Ahdida, Maria Carolina Amoedo Goncalves, Yanis An-

drebe, Oznur Apsimon, Robert Apsimon, Jordan Matthias Arnesano, Anna-Maria Bachmann, Diego Barrientos, Fabian Batsch, Vittorio Bencini, Michele Bergamaschi, Patrick Blanchard, Philip Nicholas Burrows, Birger Buttenschön, Allen Caldwell, James Chappell, Eric Chevallay, Moses Chung, David Andrew Cooke, Heiko Damerau, Can Davut, Gabor Demeter, Amos Christopher Dexter, Steffen Doeber, Francesca Ann Elverson, John Farmer, Ambrogio Fasoli, Valentin Fedosseev, Ricardo Fonseca, Ivo Forno, Spencer Gessner, Aleksandr Gorn, Eduardo Granados, Marcel Granetzny, Tim Graubner, Olaf Grulke, Eloise Daria Guran, Vasyly Hafych, Anthony Hartin, James Henderson, Mathias Hüther, Miklos Kedves, Fearghus Keeble, Vadim Khudiakov, Seong-Yeol Kim, Florian Kraus, Michel Krupa, Thibaut Lefevre, Linbo Liang, Shengli Liu, Nelson Lopes, Miguel Martinez Calderon, Stefano Mazzoni, David Medina Godoy, Joshua Moody, Kookjin Moon, Pablo Israel Morales Guzmán, Mariana Moreira, Tatiana Nechaeva, Elzbieta Nowak, Collette Pakuza, Harsha Panuganti, Ans Pardons, Kevin Pepitone, Aravinda Perera, Jan Pucek, Alexander Pukhov, Rebecca Louise Ramjiawan, Stephane Rey, Adam Scaachi, Oliver Schmitz, Eugenio Senes, Fernando Silva, Luis Silva, Christine Stollberg, Alban Sublet, Catherine Swain, Athanasios Topaloudis, Nuno Torrado, Petr Tuev, Marlene Turner, Francesco Velotti, Livio Verra, Victor Verzilov, Jorge Vieira, Helmut Vincke, Martin Weidl, Carsten Welsch, Manfred Wendt, Peerawan Wiwattananon, Joseph Wolfenden, Benjamin Woolley, Samuel Wyler, Guoxing Xia, Vlada Yarygova, Michael Zepp, and Giovanni Zevi Della Porta. The awake run 2 programme and beyond. *Symmetry*, 14(8), 2022.

[16] Gennady Plyushchev, Roberto Kersevan, Alexey Petrenko, and Patric Muggli. A rubidium vapor source for a plasma source for awake. *Journal of Physics D: Applied Physics*, 51(2):025203, 2017.

[17] F. Batsch, P. Muggli, R. Agnello, C. C. Ahdida, M. C. Amoedo Goncalves, Y. Andrebe, O. Apsimon, R. Apsimon, A.-M. Bachmann, M. A. Bastrukov, P. Blanchard, F. Braunmüller, P. N. Burrows, B. Buttenschön, A. Caldwell, J. Chappell, E. Chevallay, M. Chung, D. A. Cooke, H. Damerau, C. Davut, G. Demeter, H. L. Deubner, S. Doeber, J. Farmer, A. Fasoli, V. N. Fedosseev, R. Fiorito, R. A. Fonseca, F. Friebel, I. Forno, L. Garolfi, S. Gessner, I. Gorgisyan, A. A. Gorn, E. Granados, M. Granetzny, T. Graubner, O. Grulke, E. Gschwendtner, V. Hafych, A. Helm, J. R. Henderson, M. Hüther, I. Yu. Kargapolov, S.-Y. Kim, F. Kraus, M. Krupa, T. Lefevre, L. Liang, S. Liu, N. Lopes, K. V. Lotov, M. Martyanov, S. Mazzoni, D. Medina Godoy, V. A. Minakov, J. T. Moody, K. Moon, P. I. Morales Guzmán, M. Moreira, T. Nechaeva, E. Nowak, C. Pakuza, H. Panuganti, A. Pardons, A. Perera, J. Pucek, A. Pukhov, R. L. Ramjiawan, S. Rey, K. Rieger, O. Schmitz, E. Senes, L. O. Silva, R. Speroni, R. I. Spitsyn, C. Stollberg, A. Sublet, A. Topaloudis, N. Torrado, P. V. Tuev, M. Turner, F. Velotti, L. Verra, V. A. Verzilov, J. Vieira, H. Vincke, C. P. Welsch, M. Wendt, M. Wing, P. Wiwattananon, J. Wolfenden, B. Woolley, G. Xia, M. Zepp, and G. Zevi Della Porta. Transition between instability and seeded self-modulation of a relativistic particle bunch in plasma. *Phys. Rev. Lett.*, 126:164802, Apr 2021.

[18] Marlene Turner, Edda Gschwendtner, and Patric Muggli. A method to determine the maximum radius of defocused protons after self-modulation in awake. *Nuclear Instruments and Methods in Physics Research Section A: Accelerators, Spectrometers, Detectors and Associated Equipment*, 909:123–125, 2018.

[19] Rhon Keinigs and Michael E Jones. Two-dimensional dynamics of the plasma wakefield accelerator. *The Physics of fluids*, 30(1):252–263, 1987.

[20] L Verra, E Gschwendtner, and P Muggli. Adiabatic focusing of a long proton bunch in plasma. *arXiv preprint arXiv:2208.12342*, 2022.

[21] C Benedetti Schroeder, Carlo Benedetti, Eric Esarey, FJ Grüner, and WP Leemans. Growth and phase velocity of self-modulated beam-driven plasma waves. *Physical Review Letters*, 107(14):145002, 2011.

[22] AP Sosedkin and KV Lotov. Lcode: A parallel quasistatic code for computationally heavy problems of plasma wakefield acceleration. *Nuclear Instruments and Methods in Physics Research Section A: Accelerators, Spectrometers, Detectors and Associated Equipment*, 829:350–352, 2016.

[23] Mariana Moreira, Jorge Vieira, and Patric Muggli. Influence of proton bunch parameters on a proton-driven plasma wakefield acceleration experiment. *Physical Review Accelerators and Beams*, 22(3):031301, 2019.

[24] A A Gorn, M Turner, E Adli, R Agnello, M Aladi, Y Andrebe, O Apsimon, R Apsimon, A-M Bachmann, M A Bastrukov, F Batsch, M Bergamaschi, P Blanchard, P N Burrows, B Buttenschön, A Caldwell, J Chappell, E Chevallay, M Chung, D A Cooke, H Damerau, C Davut, G Demeter, L H Deubner, A Dexter, G P Djotyan, S Doeber, J Farmer, A Fasoli, V N Fedosseev, R Fiorito, R A Fonseca, F Friebel, I Forno, L Garolfi, S Gessner, B Goddard, I Gorgisyan, E Granados, M Granetzny, O Grulke, E Gschwendtner, V Hafych, A Hartin, A Helm, J R Henderson, A Howling, M Hüther, R Jacquier, I Yu Kargapolov, M Á Kedves, F Keeble, M D Kelisani, S-Y Kim, F Kraus, M Krupa, T Lefevre, L Liang, S Liu, N Lopes, K V Lotov, M Martyanov, S Mazzoni, D Medina Godoy, V A Minakov, J T Moody, P I Morales Guzmán, M Moreira, T Nechaeva, H Panuganti, A Pardons, F Peña Asmus, A Perera, A Petrenko, J Pucek, A Pukhov, B Ráczkevi, R L Ramjiawan, S Rey, H Ruhl, H Saberi, O Schmitz, E Senes, P Sherwood, L O Silva, R I Spitsyn, P V Tuev, F Velotti, L Verra, V A Verzilov, J Vieira, C P Welsch, B Williamson, M Wing, J Wolfenden, B Woolley, G Xia, M Zepp, G Zevi Della Porta, and The AWAKE Collaboration. Proton beam defocusing in awake: comparison of simulations and measurements. *Plasma Physics and Controlled Fusion*, 62(12):125023, nov 2020.

[25] KV Lotov, A Pukhov, and A Caldwell. Effect of plasma inhomogeneity on plasma wakefield acceleration driven by long bunches. *Physics of Plasmas*, 20(1), 2013.

[26] KV Lotov. Physics of beam self-modulation in plasma wakefield accelerators. *Physics of Plasmas*, 22(10), 2015.

[27] A. Pukhov, N. Kumar, T. Tückmantel, A. Upadhyay, K. Lotov, P. Muggli, V. Khudik, C. Siemon, and G. Shvets. Phase velocity and particle injection in a self-modulated proton-driven plasma wakefield accelerator. *Phys. Rev. Lett.*, 107:145003, Sep 2011.

[28] K V Lotov and V A Minakov. Proton beam self-modulation seeded by electron bunch in plasma with density ramp. *Plasma Physics and Controlled Fusion*,

62(11):115025, October 2020.

[29] L. Verra, G. Zevi Della Porta, J. Pucek, T. Nechaeva, S. Wyler, M. Bergamaschi, E. Senes, E. Guran, J. T. Moody, M. Á. Kedves, E. Gschwendtner, P. Muggli, R. Agnello, C. C. Ahdida, M. C. A. Goncalves, Y. Andrebe, O. Apsimon, R. Apsimon, J. M. Arnesano, A.-M. Bachmann, D. Barrientos, F. Batsch, V. Bencini, P. Blanchard, P. N. Burrows, B. Buttenschön, A. Caldwell, J. Chappell, E. Chevallay, M. Chung, D. A. Cooke, C. Davut, G. Demeter, A. C. Dexter, S. Doeberl, F. A. Elverson, J. Farmer, A. Fasoli, V. Fedosseev, R. Fonseca, I. Furno, A. Gorn, E. Granados, M. Granetzy, T. Graubner, O. Grulke, V. Hafych, J. Henderson, M. Hüther, V. Khudiakov, S.-Y. Kim, F. Kraus, M. Krupa, T. Lefevre, L. Liang, S. Liu, N. Lopes, K. Lotov, M. Martinez Calderon, S. Mazzoni, D. Medina Godoy, K. Moon, P. I. Morales Guzmán, M. Moreira, E. Nowak, C. Pakuza, H. Panuganti, A. Pardons, K. Pepitone, A. Perera, A. Pukhov, R. L. Ramjiawan, S. Rey, O. Schmitz, F. Silva, L. Silva, C. Stollberg, A. Sublet, C. Swain, A. Topaloudis, N. Torrado, P. Tuev, F. Velotti, V. Verzilov, J. Vieira, M. Weidl, C. Welsch, M. Wendt, M. Wing, J. Wolfenden, B. Woolley, G. Xia, V. Yarygova, and M. Zepp. Controlled growth of the self-modulation of a relativistic proton bunch in plasma. *Phys. Rev. Lett.*, 129:024802, Jul 2022.

[30] A. Caldwell. Collider physics at high energies and low luminosities. *The European Physical Journal Special Topics*, 223(6):1139–1143, May 2014.

[31] A. Caldwell and M. Wing. Vheep: a very high energy electron–proton collider. *The European Physical Journal C*, 76(8), 2016.

[32] M. Wing. Particle physics experiments based on the awake acceleration scheme. *Philosophical Transactions of the Royal Society A: Mathematical, Physical and Engineering Sciences*, 377(2151):20180185, June 2019.

[33] Félicie Albert, M E Couprise, Alexander Debus, Mike C Downer, Jérôme Faure, Alessandro Flacco, Leonida A Gizzi, Thomas Grismayer, Axel Huebl, Chan Joshi, M Labat, Wim P Leemans, Andreas R Maier, Stuart P D Mangles, Paul Mason, François Mathieu, Patric Muggli, Mamiko Nishiuchi, Jens Osterhoff, P P Rajeev, Ulrich Schramm, Jörg Schreiber, Alec G R Thomas, Jean-Luc Vay, Marija Vranic, and Karl Zeil. 2020 roadmap on plasma accelerators. *New Journal of Physics*, 23(3):031101, March 2021.

[34] N Lemos, J L Martins, F S Tsung, J L Shaw, K A Marsh, F Albert, B B Pollock, and C Joshi. Self-modulated laser wakefield accelerators as x-ray sources. *Plasma Physics and Controlled Fusion*, 58(3):034018, February 2016.